NeuroImage: Clinical 2 (2013) 658–662

Contents lists available at ScienceDirect

NeuroImage: Clinical

journal homepage: www.elsevier.com/locate/ynicl

Measurement of blood–brain barrier permeability in acute ischemic stroke using standard first-pass perfusion CT data☆

Giang Truong Nguyen [a], Alan Coulthard [b,c], Andrew Wong [d], Nabeel Sheikh [d], Robert Henderson [d], John D. O'Sullivan [d], David C. Reutens [a,d,*]

[a] Centre for Advanced Imaging, The University of Queensland, Australia
[b] Academic Discipline of Medical Imaging, The University of Queensland, Australia
[c] Department of Medical Imaging, Royal Brisbane & Women's Hospital, Brisbane Australia
[d] Department of Neurology, Royal Brisbane & Women's Hospital, Brisbane, Australia

ARTICLE INFO

Article history:
Received 15 January 2013
Received in revised form 1 April 2013
Accepted 10 April 2013
Available online 22 April 2013

Keywords:
Perfusion CT
Blood–brain barrier permeability
First-pass
Delayed phase

ABSTRACT

Background and purpose: Increased blood–brain barrier permeability is believed to be associated with complications following acute ischemic stroke and with infarct expansion. Measurement of blood–brain barrier permeability requires a delayed image acquisition methodology, which prolongs examination time, increasing the likelihood of movement artefacts and radiation dose. Existing quantitative methods overestimate blood–brain barrier permeability when early phase CT perfusion data are used. The purpose of this study is to develop a method that yields the correct blood–brain barrier permeability value using first-pass perfusion CT data.

Methods: We acquired 43 CT perfusion datasets, comprising experimental ($n = 30$) and validation subject groups ($n = 13$). The Gjedde–Patlak method was used to estimate blood–brain barrier permeability using first-pass (30–60 s after contrast administration) and delayed phase (30–200 s) data. In the experimental group, linear regression was used to obtain a function predicting first-pass blood–brain barrier permeability estimates from delayed phase estimates in each stroke compartment. The reliability of prediction with this function was then tested using data from the validation group.

Results: The predicted delayed phase blood–brain barrier permeability was strongly correlated with the measured delayed phase value ($r = 0.67$ and 0.6 for experimental and validation group respectively; $p < 0.01$). Predicted and measured delayed phase blood–brain barrier permeability in each stroke compartment were not significantly different in both experimental and validation groups.

Conclusion: We have developed a method of estimating blood–brain barrier permeability using first-pass perfusion CT data. This predictive method allows reliable blood–brain barrier permeability estimation within standard acquisition time, minimizing the likelihood of motion artefacts thereby improving image quality and reducing radiation dose.

1. Introduction

Increased blood–brain barrier permeability, one of the pathological changes following ischemic stroke (Taheri et al., 2009), is believed to predispose to complications such as hemorrhagic transformation (Hamann et al., 1996), massive vasogenic oedema (Klatzo, 1987), infarct expansion (Bektas et al., 2010) and poor clinical outcome (Warach and Latour, 2004). Changes in blood–brain barrier permeability may occur spontaneously following acute stroke or may be a consequence of recanalisation therapy (Cruz-Flores et al., 2001; Molina et al., 2002, 2001; B. Thanvi et al., 2008; B.R. Thanvi et al., 2008; Treadwell and Thanvi, 2010). Because of the consequences of blood–brain barrier breakdown, there is increasing interest in the measurement of blood–brain barrier permeability in patients with acute stroke (Aoki et al., 2002; Bang et al., 2007; Lampl et al., 2006; Wang and Lo, 2003). Perfusion CT is used increasingly in the investigation of acute ischemic stroke and can be used to quantify blood–brain barrier permeability with the application of the Gjedde–Patlak plot (Gjedde, 1981, 1982; Patlak et al., 1983; Patlak and Blasberg, 1985), which is a model independent technique for the estimation of unidirectional clearance of tracers (in this case iodinated contrast agent) across the vascular endothelium in the brain. In early studies using first-pass perfusion CT data, increased blood–brain barrier permeability was found to predict the risk of hemorrhagic transformation (Lin et al.,

* Corresponding author at: Centre for Advanced Imaging, Building 60, The University of Queensland, Brisbane, QLD 4072, Australia. Tel.: +61 7 3365 4237; fax: +61 7 3365 3833.
E-mail address: d.reutens@cai.uq.edu.au (D.C. Reutens).

2213-1582/$ – see front matter © 2013 The Authors. Published by Elsevier Inc. All rights reserved.
http://dx.doi.org/10.1016/j.nicl.2013.04.004

2007). However, subsequent comparisons between blood–brain barrier permeability estimates obtained with the first-pass and delayed phases of perfusion CT data by Dankbaar et al. (2008) suggested that the use of first-pass data leads to overestimation of permeability (Hom et al., 2009). Delayed perfusion CT acquisitions lasting up to 4 min have the disadvantages of a greater likelihood of artefacts due to patient movement and of increased radiation dose (Schneider et al., 2011).

In this study we examined the correlation between blood–brain barrier permeability estimates obtained from the terminal phase of a first-pass acquisition and from delayed phase data. The terminal phase of a first-pass acquisition contains information from the early period of contrast recirculation. We then developed a method of predicting delayed phase blood–brain barrier permeability estimates using estimates from first-pass data and validated the predictive model in a second cohort of acute stroke patients.

2. Methods

2.1. Patients

Forty three patients admitted with a clinical diagnosis of acute ischemic stroke to Royal Brisbane and Women's Hospital were recruited between May 2011 and April 2012. All patients underwent perfusion CT study at admission. Thirty perfusion CT datasets were randomly selected and comprised the experimental group while the remaining 13 subjects comprised the validation group for the study (selected without regard for age or gender). This research project was approved by the hospital's Human Research Ethics Committee.

2.2. Perfusion CT imaging

Patients underwent perfusion CT examination on a 128-slice CT scanner (Siemens Somatom Definition AS+ Siemens AG Erlangen Germany). Images were acquired in cine mode with multiple gantry rotations starting at 6 s after intravenous administration of 40 ml of iodinated contrast agent (Ultravist 300 mgI/ml; Bayer HealthCare Pharmaceutical Inc., Leverkusen, Germany) at a flow rate of 6 ml/s via an 18-Gauge catheter inserted into an antecubital vein. Image acquisition included first-pass (26 scans over 60 s) and delayed-phase (four contiguous scans lasting 140 additional seconds beginning at 80, 120, 160 and 200 s). Scans were performed with a tube voltage of 120 kVp, a tube current of 80 mA, slice-thickness of 3 mm, and Z-axis coverage of 90 mm from the skull base to the vertex.

2.3. Perfusion CT analysis

Automated motion correction between time frames was performed using FLIRT (FSL-FMRIB, Oxford UK). Image noise was then removed and vascular structures were identified with independent components analysis using MELODIC (FSL-FMRIB). From the arterial component map created with independent component analysis, the pre-bifurcation segment (M1) of the middle cerebral artery contralateral to the affected cerebral hemisphere was manually segmented by a trained observer (GTN). The arterial input function was obtained as the mean value in Hounsfield units from all voxels in the segmented M1 in each time frame (Ferreira et al., 2010). Voxel-based maps of cerebral blood flow, cerebral blood volume, and mean transit time were generated with purpose-written software using MATLAB R2012a (The MathWorks Inc., Natick, USA). Cerebral blood flow maps were created by deconvolution using the standard singular value decomposition approach (Konstas et al., 2009a; Ostergaard et al., 1996). Cerebral blood volume was calculated as the ratio between the area under the tissue time-intensity curve and the area under the arterial input function. Mean transit time maps were then created as the ratio between cerebral blood volume and cerebral blood flow (Konstas et al., 2009a, 2009b). Stroke compartments were defined as penumbra (tissue-at-risk), infarct core (not salvageable tissue), and entire ischemic tissue (penumbra plus infarct core). Infarct core and tissue-at-risk compartments were segmented by applying the following cerebral blood volume and mean transit time thresholds: a. Penumbra: mean transit time > 145% compared to contralateral region and cerebral blood volume ≥ 2.0 ml/100 g; b. Infarct core: mean transit time > 145% and cerebral blood volume < 2.0 ml/100 g (Wintermark et al., 2006). Using these thresholds, we generated volumes of interest corresponding to penumbra, infarct core and entire ischemic tissue. Volumes of interest corresponding to non-stroke tissue were generated as mean value of a region of interest created by reflecting the entire ischemic volume of interest across the midline.

2.4. Estimation of blood–brain barrier permeability

Blood–brain barrier permeability values were estimated from perfusion CT data using the Gjedde–Patlak method (Fig. 1) (Gjedde, 1981, 1982; Patlak et al., 1983; Patlak and Blasberg, 1985):

$$\frac{M_t(t)}{C_a(t)} = K_1 * \frac{\int_0^t C_a(\tau)d\tau}{C_a(t)} + Vp$$

where M_t is image intensity (measured in Hounsfield units) in each brain tissue voxel at time t; $C_a(t)$ is mean intensity from all voxels in the M1 segment at time t (measured in Hounsfield units); K_1 is the transfer coefficient for unidirectional clearance of contrast agent across the endothelial membrane, a measure of blood − brain barrier permeability; and Vp denotes the vascular space from which clearance occurs. The least squares estimate of K_1 was obtained at each voxel using linear regression. Blood − brain barrier permeability was estimated using both first-pass (K_1^{FP}, 30 − 60 s after intravenous contrast administration), and delayed-phase (K_1^{DP}, 60 − 200 s) data. Mean K_1^{FP} and K_1^{DP} values in each volume of interest were then calculated. To evaluate the quality of graphical analysis, the root-mean-square error of the Gjedde − Patlak plot was calculated at voxel level and normalised by the mean value of $M_t(t)$ / $C_a(t)$ for each measurement time frame. The mean difference in normalised root-mean-square errors for each time frame was compared assessed for each stroke compartment.

2.5. Statistical analysis

The paired t-test was used to compare K_1^{FP} and measured K_1^{DP} and to compare normalised root-mean-square errors. We used the Bonferroni correction for multiple comparisons. In the experimental group, analysis of covariance was performed to examine whether the relationship between K_1^{FP} and K_1^{DP} differed between stroke compartments. Linear

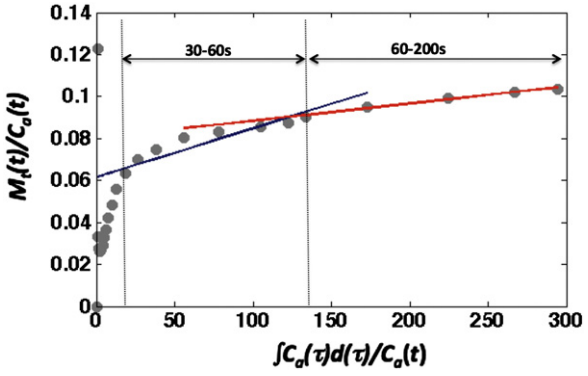

Fig. 1. Example of Gjedde–Patlak plot in one subject using mean intensity values in the entire ischemic region and in the M1 segment of the middle cerebral artery. The slope of the plot is lower for the 60–200 s time frame than the 30–60s time frame. A better linear fit is seen for the 60–200 s time frame.

Table 1
Subject demographics and clinical information.

	Experimental group	Validation group
Age: Mean ± standard deviation	69 ± 16 years	71 ± 12 years
Gender		
Male	13 (43%)	8 (61%)
Female	17 (57%)	5 (39%)
Diagnosis		
Transient ischemic attack	7 (23%)	8 (62%)
Anterior cerebral artery (ACA) stroke	2 (7%)	–
Middle cerebral artery (MCA) stroke	17 (57%)	5 (38%)
Anterior choroidal artery stroke	2 (7%)	–
Posterior cerebral artery stroke	1 (3%)	–
MCA + ACA stroke	1 (3%)	–
Volume: Median (range)		
Penumbra	62 (1–211 ml)	74 (2–140 ml)
Infarct core	9 (0.4–78 ml)	17 (0.5–25 ml)
Time between onset and CT: Mean ± standard deviation	2.8 ± 1.2 h	3.7 ± 2.3 h
Thrombolysis	9 (30%)	4 (31%)
Thrombectomy	2 (7%)	–

regression between K_1 estimates from the two time frames in all compartments was used to generate a model predicting K_1^{DP} from K_1^{FP} estimates. Predicted K_1^{DP} values were then generated in each voxel using the predictive model. Mean predicted K_1^{DP} values were calculated for each volume of interest in both the experimental and the validation group. In both groups mean predicted and measured K_1^{DP} were compared using the paired *t*-test. To test the accuracy of the prediction method, prediction regression error sum of squares, mean square error of prediction, and goodness of fit (R^2) were calculated in both groups.

3. Results

3.1. Subjects

Forty-three patients (22 Males, 21 Females) were enrolled in the study. Mean age was 70 years (range: 42 to 93 years). Perfusion CT scans were performed one to seven hours after stroke onset (mean ± standard deviation: 3 ± 1.5 h). Twenty-eight patients had a clinically confirmed ischemic stroke, while 15 patients were diagnosed as having a transient ischemic attack because clinical symptoms resolved within 24 h and no infarct was seen on follow up MRI. The features of the patients in the experimental and validation groups are shown in Table 1.

3.2. Relationship between K_1^{DP} and K_1^{FP}

Mean K_1^{FP} was significantly higher than measured K_1^{DP} in all tissue compartments ($p < 0.0001$; Table 2). Analysis of covariance revealed no significant interaction between stroke compartment and the covariance between K_1^{DP} and K_1^{FP} ($F = 0.95$, $p = 0.42$). In light of this, a linear predicting function was generated from the regression between mean K_1^{DP} and K_1^{FP} values in each stroke and non-stroke compartment for each subject:

$$Predicted\,K_1^{DP} = 0.16 \times K_1^{FP} + 1.74.$$

Standard errors of the slope and intercept were 0.02 and 0.16 respectively. K_1^{DP} values in patients with transient ischemic attacks were similar to those for non-stroke tissue in stroke patients.

3.2.1. Relationship between predicted and measured K_1^{DP}

Predicted and measured K_1^{DP} estimates were strongly correlated in both the experimental group ($r = 0.67$, $p < 0.01$) and the validation group ($r = 0.60$, $p < 0.01$) as shown in Fig. 2. A typical image of measured and predicted K_1^{DP} is shown in Fig. 3.

3.2.2. Quality of the Gjedde–Patlak model fit

The mean normalised root-mean-square error for plots utilising data from each time frame are shown in Table 3. The mean normalised root mean square error was significantly higher for first-pass data than for delayed phase data.

3.2.3. Comparison between predicted and measured K_1^{DP}

The mean value of predicted K_1^{DP} in each volume of interest did not differ significantly from the measured value (Table 1) in both the experimental and validation groups with $p > 0.05$ in all comparisons.

3.3. Reliability of the prediction method

In the experimental group, the predicting function explained 45% of the variance in K_1^{DP} ($R^2 = 0.45$, $F(1, 97) = 80.5$, $p < 0.01$). In the validation group, K_1^{FP} explained 35% of the variance ($R^2 = 0.35$, $F(1, 27) = 14.4$, $p < 0.01$). Prediction regression sum of square error in the experimental group (69.6) was greater than in the validation group (20.5) while the mean square error of prediction in the two datasets was similar (0.72 and 0.76 for experimental and validation groups respectively).

4. Discussion

In this study we have established a linear relationship between K_1^{FP} and K_1^{DP} in all stroke compartments. Using our model, the predicted delayed phase value was comparable to measured K_1^{DP}. Our model should assist the assessment of blood–brain barrier permeability in acute stroke by removing the requirement for prolonged perfusion CT acquisitions.

Although early studies used the first-pass perfusion CT data to assess permeability changes (Lin et al., 2007; Cianfoni et al., 2006), Hom et al. (2009) found that the optimal acquisition time to estimate blood–brain barrier permeability using the Gjedde–Patlak plot was at least 210 s after intravenous contrast injection. At earlier time points, the Gjedde–Patlak plot is not linear resulting in overestimation of blood–brain barrier permeability (Dankbaar et al., 2008). Like previous authors we observed that K_1 estimates were lower for delayed phase compared to first-pass data. To minimize overestimation when first-pass perfusion

Table 2
K_1^{DP} and measured and predicted K_1^{DP} in experimental and validation groups.

Stroke sub-region	Experimental group (Mean ± SD)			Validation group (Mean ± SD)		
	K_1^{FP} †	Measured K_1^{DP} †	Predicted K_1^{DP} †	K_1^{FP}	Measured K_1^{DP}	Predicted K_1^{DP}
Penumbra	9.4 ± 5.6	3.37 ± 1.16	3.24 ± 0.92	9.6 ± 7.5	3.63 ± 0.89	3.27 ± 1.19
Infarct	7.0 ± 3.9	2.97 ± 1.18	2.85 ± 0.63	8.7 ± 5.7	3.53 ± 0.87	3.12 ± 0.91
Entire ischemic tissue	9.0 ± 5.1	3.30 ± 1.15	3.17 ± 0.82	9.3 ± 7.2	3.57 ± 0.90	3.22 ± 1.14
Non-stroke tissue	6.4 ± 3.8	2.51 ± 0.90	2.77 ± 0.60	6.5 ± 2.3	2.41 ± 0.97	2.77 ± 0.36
All compartments	8.4 ± 5.0	2.99 ± 1.13	2.99 ± 0.77	8.0 ± 5.2	3.05 ± 1.05	3.02 ± 0.28

SD: Standard deviation.
† ml/100 g/min.

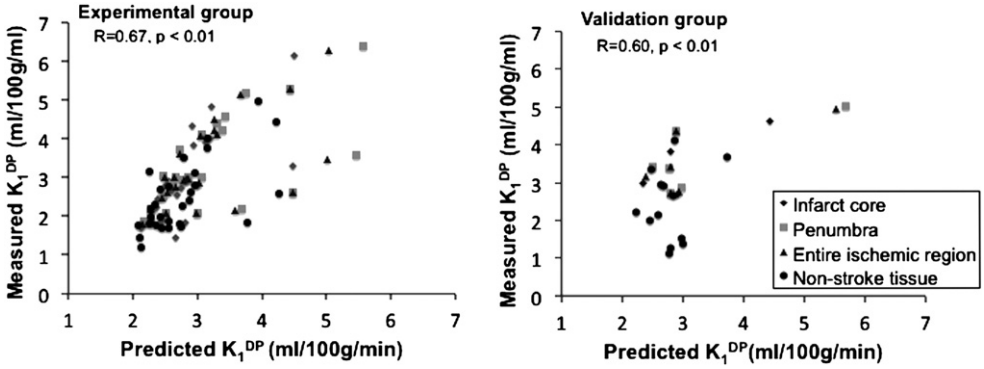

Fig. 2. Relationship between predicted K_1^{DP} and measured K_1^{DP} in all stroke compartments. Results for the experimental group are shown on the left and for the validation group on the right.

CT data are used, Schneider et al. (2011) attempted to correct for delays in arrival time of the contrast bolus shifting the peak of the arterial input function to match that of the tissue enhancement curve in each voxel of an image. This approach still required acquisitions of up to 90 s in length rather than using standard first-pass data alone because of lack of equilibrium conditions.

Dankbaar et al. (2008) pointed out that the Gjedde–Patlak plots constructed from first-pass data are not linear, especially for tissue at risk because of delayed enhancement in the tissue at risk compared with the arterial input function and preserved or increased intensity of the enhancement in the tissue at risk. This causes the Gjedde–Patlak plot to rise steeply during the first-pass and fall steeply at the end of the first-pass. It should be emphasized that in our study, the time frame from 30 to 60 s after contrast administration was used to estimate K_1 in the first-pass data because this was after the negatively sloping part of the plot and at the start of the second positive slope of the Gjedde–Patlak plot in relation to contrast recirculation. Dankbaar et al. (2008) suggested that blood–brain barrier permeability values measured from the first-pass and from the delayed phase do not differ as much in the infarct core as they do in the tissue at risk. The accuracy of predicting K_1 values did not differ significantly between stroke compartments. Predicted values did not differ from measured K_1^{DP} in any of the tissue compartments and values were comparable with previously published blood–brain barrier permeability values (Lin et al., 2007; Hom et al., 2009; Dankbaar et al., 2011). The predicting function developed in the present study was for data obtained in specific measurement time frames. However, the approach should be applicable to obtaining predicting functions using data from other acquisition protocols.

The quality of the fit in the Gjedde–Patlak plots, assessed with the mean normalised root-mean-square error of the fit in each stroke compartment, suggested a significantly better linear fit in the delayed phase. With the use of standard first-pass perfusion CT data, the acquisition time of the images required to estimate blood–brain barrier permeability is significantly reduced compared to delayed image acquisition (60 instead of 200 s). This minimizes risk of motion artefacts, which are often seen in delayed images prior to registration. Recent publications have highlighted the radiation exposure from comprehensive CT evaluation of acute stroke, the possibility of radiation induced sequela with repetitive examinations and the need to consider the potential risk-benefit ratio for new techniques (Latchaw et al., 2009; Mnyusiwalla et al., 2009). The effective radiation dose for the prolonged acquisition in this study was

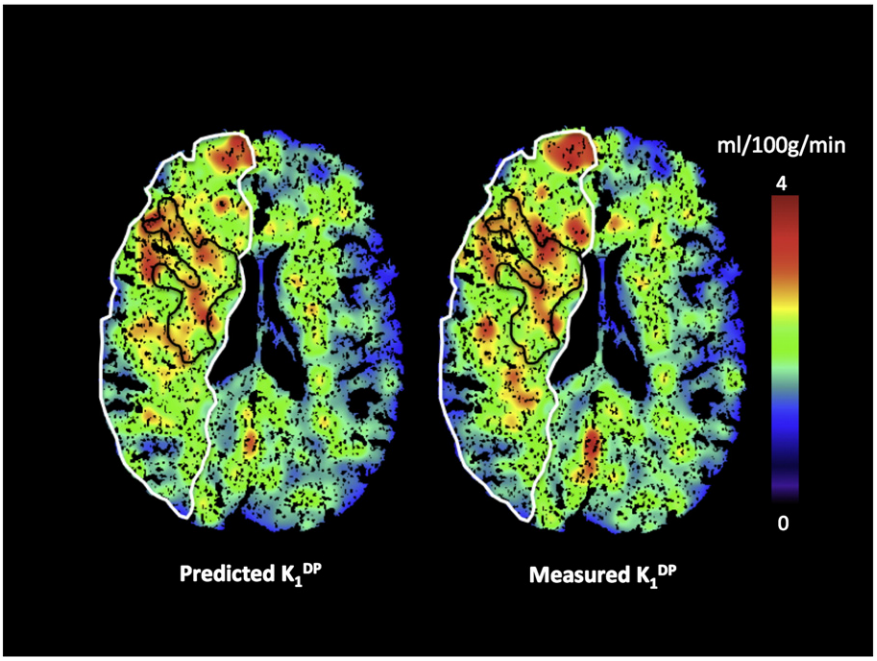

Fig. 3. Images of predicted and measured K_1^{DP} showing increased blood–brain barrier permeability in the ischemic region (white boundary) and infarct core (black boundary) compared to the homologous regions in the unaffected contralateral hemisphere.

Table 3
Mean normalised root-mean-square error (±standard deviation) for graphical analysis in each stroke compartment.

Stroke compartment	First pass	Delayed phase	
Penumbra	0.78 ± 0.08	0.67 ± 0.06	$p < 0.0001$
Infarct core	0.85 ± 0.13	0.69 ± 0.09	$p < 0.0001$
Non-stroke tissue	0.77 ± 0.1	0.64 ± 0.08	$p < 0.0001$

5.2 mSv compared to 4.5 mSv for the first-pass acquisition, a reduction of 14% in effective radiation dose.

5. Conclusion

Our model predicts delayed blood–brain barrier permeability using first-pass perfusion CT data in patients following acute stroke. By using first-pass data, scanning time is not prolonged thus reducing radiation exposure and lessening the likelihood of motion artefacts. The sample size for both groups was relatively small and future studies with larger samples and different scanning protocols would address the generalizability of our method and its ability to predict stroke complications such as haemorrhage and oedema.

Disclosures

None.

References

Aoki, T., Sumii, T., Mori, T., Wang, X., Lo, E.H., 2002. Blood–brain barrier disruption and matrix metalloproteinase-9 expression during reperfusion injury: mechanical versus embolic focal ischemia in spontaneously hypertensive rats. Stroke 33, 2711–2717.

Bang, O.Y., Buck, B.H., Saver, J.L., Alger, J.R., Yoon, S.R., Starkman, S., Ovbiagele, B., Kim, D., Ali, L.K., Sanossian, N., Jahan, R., Duckwiler, G.R., Vinuela, F., Salamon, N., Villablanca, J.P., Liebeskind, D.S., 2007. Prediction of hemorrhagic transformation after recanalization therapy using T2*-permeability magnetic resonance imaging. Annals of Neurology 62, 170–176.

Bektas, H., Wu, T.C., Kasam, M., Harun, N., Sitton, C.W., Grotta, J.C., Savitz, S.I., 2010. Increased blood–brain barrier permeability on perfusion CT might predict malignant middle cerebral artery infarction. Stroke 41, 2539–2544.

Cianfoni, A., Cha, S., Bradley, W.G., Dillon, W.P., Wintermark, M., 2006. Quantitative measurement of blood–brain barrier permeability using perfusion-CT in extra-axial brain tumors. Journal of Neuroradiology 33, 164–168.

Cruz-Flores, S., Thompson, D.W., Boiser, J.R., 2001. Massive cerebral edema after recanalization post-thrombolysis. Journal of Neuroimaging 11, 447–451.

Dankbaar, J.W., Hom, J., Schneider, T., Cheng, S.C., Lau, B.C., van der Schaaf, I., Virmani, S., Pohlman, S., Dillon, W.P., Wintermark, M., 2008. Dynamic perfusion CT assessment of the blood–brain barrier permeability: first pass versus delayed acquisition. American Journal of Neuroradiology 29, 1671–1676.

Dankbaar, J.W., Hom, J., Schneider, T., Cheng, S.C., Bredno, J., Lau, B.C., van der Schaaf, I.C., Wintermark, M., 2011. Dynamic perfusion-CT assessment of early changes in blood brain barrier permeability of acute ischaemic stroke patients. Journal of Neuroradiology 38, 161–166.

Ferreira, R.M., Lev, M.H., Goldmakher, G.V., Kamalian, S., Schaefer, P.W., Furie, K.L., Gonzalez, R.G., Sanelli, P.C., 2010. Arterial input function placement for accurate CT perfusion map construction in acute stroke. AJR. American Journal of Roentgenology 194, 1330–1336.

Gjedde, A., 1981. High- and low-affinity transport of D-glucose from blood to brain. Journal of Neurochemistry 36, 1463–1471.

Gjedde, A., 1982. Calculation of cerebral glucose phosphorylation from brain uptake of glucose analogs in vivo: a re-examination. Brain Research 257, 237–274.

Hamann, G.F., Okada, Y., del Zoppo, G.J., 1996. Hemorrhagic transformation and microvascular integrity during focal cerebral ischemia/reperfusion. Journal of Cerebral Blood Flow and Metabolism 16, 1373–1378.

Hom, J., Dankbaar, J.W., Schneider, T., Cheng, S.C., Bredno, J., Wintermark, M., 2009. Optimal duration of acquisition for dynamic perfusion CT assessment of blood–brain barrier permeability using the Patlak model. American Journal of Neuroradiology 30, 1366–1370.

Klatzo, I., 1987. Pathophysiological aspects of brain edema. Acta Neuropathologica 72, 236–239.

Konstas, A.A., Goldmakher, G.V., Lee, T.Y., Lev, M.H., 2009a. Theoretic basis and technical implementations of CT perfusion in acute ischemic stroke, part 1: theoretic basis. AJNR. American Journal of Neuroradiology 30, 662–668.

Konstas, A.A., Goldmakher, G.V., Lee, T.Y., Lev, M.H., 2009b. Theoretic basis and technical implementations of CT perfusion in acute ischemic stroke, part 2: technical implementations. AJNR. American Journal of Neuroradiology 30, 885–892.

Lampl, Y., Sadeh, M., Lorberboym, M., 2006. Prospective evaluation of malignant middle cerebral artery infarction with blood–brain barrier imaging using Tc-99m DTPA SPECT. Brain Research 1113, 194–199.

Latchaw, R.E., Alberts, M.J., Lev, M.H., Connors, J.J., Harbaugh, R.E., Higashida, R.T., Hobson, R., Kidwell, C.S., Koroshetz, W.J., Mathews, V., Villablanca, P., Warach, S., Walters, B., 2009. Recommendations for imaging of acute ischemic stroke: a scientific statement from the American Heart Association. Stroke 40, 3646–3678.

Lin, K., Kazmi, K.S., Law, M., Babb, J., Peccerelli, N., Pramanik, B.K., 2007. Measuring elevated microvascular permeability and predicting hemorrhagic transformation in acute ischemic stroke using first-pass dynamic perfusion CT imaging. American Journal of Neuroradiology 28, 1292–1298.

Mnyusiwalla, A., Aviv, R.I., Symons, S.P., 2009. Radiation dose from multidetector row CT imaging for acute stroke. Neuroradiology 51, 635–640.

Molina, C.A., Montaner, J., Abilleira, S., Ibarra, B., Romero, F., Arenillas, J.F., Alvarez-Sabin, J., 2001. Timing of spontaneous recanalization and risk of hemorrhagic transformation in acute cardioembolic stroke. Stroke 32, 1079–1084.

Molina, C.A., Alvarez-Sabin, J., Montaner, J., Abilleira, S., Arenillas, J.F., Coscojuela, P., Romero, F., Codina, A., 2002. Thrombolysis-related hemorrhagic infarction: a marker of early reperfusion, reduced infarct size, and improved outcome in patients with proximal middle cerebral artery occlusion. Stroke 33, 1551–1556.

Ostergaard, L., Weisskoff, R.M., Chesler, D.A., Gyldensted, C., Rosen, B.R., 1996. High resolution measurement of cerebral blood flow using intravascular tracer bolus passages. Part I: mathematical approach and statistical analysis. Magnetic Resonance in Medicine 36, 715–725.

Patlak, C.S., Blasberg, R.G., 1985. Graphical evaluation of blood-to-brain transfer constants from multiple-time uptake data. Generalizations. Journal of Cerebral Blood Flow and Metabolism 5, 584–590.

Patlak, C.S., Blasberg, R.G., Fenstermacher, J.D., 1983. Graphical evaluation of blood-to-brain transfer constants from multiple-time uptake data. Journal of Cerebral Blood Flow and Metabolism 3, 1–7.

Schneider, T., Hom, J., Bredno, J., Dankbaar, J.W., Cheng, S.C., Wintermark, M., 2011. Delay correction for the assessment of blood–brain barrier permeability using first-pass dynamic perfusion CT. American Journal of Neuroradiology 32, E134–E138.

Taheri, S., Candelario-Jalil, E., Estrada, E.Y., Rosenberg, G.A., 2009. Spatiotemporal correlations between blood–brain barrier permeability and apparent diffusion coefficient in a rat model of ischemic stroke. PLoS One 4, e6597.

Thanvi, B., Treadwell, S., Robinson, T., 2008a. Early neurological deterioration in acute ischaemic stroke: predictors, mechanisms and management. Postgraduate Medical Journal 84, 412–417.

Thanvi, B.R., Treadwell, S., Robinson, T., 2008b. Haemorrhagic transformation in acute ischaemic stroke following thrombolysis therapy: classification, pathogenesis and risk factors. Postgraduate Medical Journal 84, 361–367.

Treadwell, S.D., Thanvi, B., 2010. Malignant middle cerebral artery (MCA) infarction: pathophysiology, diagnosis and management. Postgraduate Medical Journal 86, 235–242.

Wang, X., Lo, E.H., 2003. Triggers and mediators of hemorrhagic transformation in cerebral ischemia. Molecular Neurobiology 28, 229–244.

Warach, S., Latour, L.L., 2004. Evidence of reperfusion injury, exacerbated by thrombolytic therapy, in human focal brain ischemia using a novel imaging marker of early blood–brain barrier disruption. Stroke 35, 2659–2661.

Wintermark, M., Flanders, A.E., Velthuis, B., Meuli, R., van Leeuwen, M., Goldsher, D., Pineda, C., Serena, J., van der Schaaf, I., Waaijer, A., Anderson, J., Nesbit, G., Gabriely, I., Medina, V., Quiles, A., Pohlman, S., Quist, M., Schnyder, P., Bogousslavsky, J., Dillon, W.P., Pedraza, S., 2006. Perfusion-CT assessment of infarct core and penumbra: receiver operating characteristic curve analysis in 130 patients suspected of acute hemispheric stroke. Stroke 37, 979–985.